MATHEMATICAL MODELING OF NON-STATIONARY THERMAL STATE OF THE PROCESSED METAL DURING ITS LASER HARDENING

Elena Naprimerova[1], Igor Yachikov[1], Yuliya Latfulina[1], Marina Samodurova[1], Evgeny Trofimov[1], Sergey Lezhnev[1], Sergey Efremov[2], Evgeniy Panin[1]

[1]South Ural State University, Chelyabinsk, Russia, sergey_legnev@mail.ru (S.L.); naprimerovaed@susu.ru (E.N.); iachikovim@susu.ru (I.Y.); latfulinays@susu.ru (Y.L.); samodurovamn@susu.ru (M.S.); trofimovea@susu.ru (E.T.); cooper802@mail.ru (E.P.)
[2]Al-Farabi Kazakh National University, Almaty, Kazakhstan, efremsa@mail.ru (S.E.)

Received 30 June 2024
Accepted 24 July 2024
DOI: 10.59957/jctm.v60.i1.2025.12

ABSTRACT

Laser hardening is used for surface hardening of wear parts. Laser equipment is suitable for hardening small and geometrically complex elements. The hardening depth is 0.1 - 1.5 mm. Experimental studies using the robot KUKA KR120 have shown that the process of laser hardening does not always lead to positive results under certain conditions of parts processing, so there is a need to create a calculation base for rational choice of parameters of the process. On the basis of the considered assumptions and limitations, a mathematical model is formulated, which is a boundary value problem for calculating the unsteady thermal state of a metal plate and determining the depth of its heating and possible penetration when the laser beam moves along its surface. A numerical algorithm is proposed that allows to approximate solve the boundary value problem of the plate warm state, to determine the depth of the hardened layer and rational parameters of metal cooling. The calculation of non-stationary temperature fields in a 40X steel plate when exposed to a laser beam with two modes of cooling it with water is shown. The depth of metal penetration and the depth of its hardening are determined.

Keywords: laser hardening, mathematical modeling, non-stationary thermal state, composite coatings.

INTRODUCTION

Currently, there is a method of surface hardening of metal products by heating the metal with a laser beam to a certain temperature and then rapidly cooling the metal due to heat dissipation into the solid part and the use of cooling fluids. Heat treatment of materials by laser does not require preheating of the part and in some cases special cooling. The metal object is placed in a machine, which is a robotic unit in which the processed element is exposed to the beam. Modern laser units can be equipped with productive cooling systems.

A steel plate was used as the investigated sample, steel grade - 40X (AISI 5140H), dimensions are 50 x 50 x 6 mm. The steel plate was hardened using a KUKA KR120 robotic unit, laser power was $P_H = 1.0 - 1.5$ kW with a spot diameter of $d_f = 2 - 3$ mm (Fig. 1). Beam scanning was carried out according to the strategy of parallel lines at a speed of $W_H = 8 - 14$ mm s with a line spacing of $\delta = 4 - 6$ mm (Fig. 2). Experimental studies have shown that the process of laser quenching does not always lead to positive results, so there is a need to create a calculation base for rational choice of parameters of the process realization.

In the literature, quite a large number of works are devoted to modeling processes in laser welding, for example [1 - 3]. Part of the work is devoted to the study of thermal processes under the influence of laser radiation. For example, a nonlinear mathematical model of heating a two-layer body is considered, taking into account the finite velocity of heat propagation and the temperature dependence of the properties of materials [4]. A numerical solution of the nonlinear hyperbolic thermal conductivity problem is obtained for the case

Fig. 1. Laser hardening of steel plate.

when the absorption of laser radiation energy is modeled by a volumetric heat source.

It was shown that only a small part of the supplied laser energy (about 1 - 15 %) is used for quenching and the greatest efficiency is achieved when melting of the surface is simply avoided [5]. A comparative study has shown that pulsed lasers are more efficient in using energy for quenching than a continuous wave laser. Similarly, the efficiency of a high-power laser turns out to be higher than that of a low-power one, and an increase in beam absorption ensures higher quenching efficiency.

The laser beam is a high-intensity energy source, so processing can be carried out with or without partial melting of the metal surface. It is desirable to avoid the effect of surface melting, and it is necessary to choose the quenching temperature at a given depth for pre-eutectoid steels (carbon content in steel less than 0.8 %) Δh by the formula $T_{quen} = A_{C3} + \Delta t_p$, where the overheating from the critical point is $\Delta t_p = 30 - 50°C$. For 40X steel the point $A_{C3} = 782°C$.

To determine the temperature distribution in the area of the focal spot under the influence of the heat flux q arising under the action of the laser beam, the formula of one-dimensional distribution of the temperature field in a semi-infinite body in the *x* direction (deep into the substrate) is most often used [6]:

$$t(x,\ \tau) - t_0 = \frac{2q}{\lambda}\sqrt{a\tau}\cdot ierfc\left[\frac{x}{2\sqrt{a\tau}}\right],$$

where τ - time; $\alpha = \lambda/(c\rho)$ - coefficient of thermal diffusivity; t_0 - initial substrate temperature.

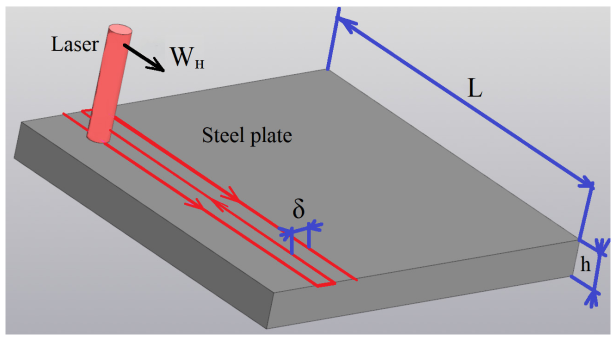

Fig. 2. Laser head scanning while heating a steel plate for hardening.

However, this formula is of a purely evaluative nature and does not take into account the entire diversity of the process: the movement of the laser spot, heat propagation through the material in horizontal directions, melting of the metal, its cooling, etc.

The process of heating and unwanted melting of steel is quite complex and depends on its thermophysical properties and a variety of geometric and technological parameters. To predict the behavior of the process under consideration, it is necessary to at least qualitatively establish how the heating depth depends on the laser beam power, its focal diameter, speed and strategy of its movement along the part surface.

There is a problem associated with the correct choice of technological modes of laser heating in the formation of the desired hardening layer on the surface of the steel part, which is usually 0.1 - 1.5 mm.

The aim of the work is to develop a mathematical model and an algorithm for calculating the non-stationary thermal state of a metal steel plate and determining the depth of its heating and possible penetration under laser exposure to obtain a high-quality quenching layer of specified dimensions.

EXPERIMENTAL

Let us consider the basic assumptions and limitations of the mathematical model.

1. Let us assume that there is a horizontal metal plate with dimensions LxL and height h. Let us choose the Cartesian coordinate system (Oxyz) as shown in Fig. 3.

2. The center of the focal spot of the laser with diameter $d_f = 2r_f$ moves along the upper surface of the plate along the Oy axis from the initial point $A_1(0, r_f, r_f)$ with velocity $W_н$. When moving from left to right, the coordinate of the spot center is given as $y_f(\tau) = r_f + W_H.\tau$, where τ is the time from the start of the motion. The time for one pass is $\tau_k = (L - 2r_f)/W_H$. The focal spot center coordinate at the end of the first pass is $B_1(0, L\text{-}r_f, r_f)$. The laser beam moves along the strategy of parallel lines with step δ. We consider that the beam moves quickly to the next line and moves from right to left from point $B_2(0, L\text{-}r_f, r_f+\delta)$ to point $A_2(0, r_f, r_f+\delta)$. Then the beam quickly passes to the next line moving from left to right starting from point $A_3(0, r_f, r_f+2\delta)$ etc. making p_0 passes.

Knowing the current time from the start of heating it is possible to determine the laser pass (line) number as $p=int(\tau/\tau_k)+1$, as well as the coordinates of the focal spot center as a function of the pass (time) number:

$$y_f = \begin{cases} r_f + \tau \cdot W_H \text{, at } p \bmod 2=1 \\ L - r_f - \tau \cdot W_H \text{, at } p \bmod 2=0 \end{cases},$$

$z_f = r_f + (p - 1).\delta$, where $p = 1, 2,\ldots p_0$.

3. We assume that the temperature field of the plate depends on time (the field is non-stationary $\partial T/\partial\tau \neq 0$). At the initial moment of time ($\tau = 0$) the plate has a temperature t_0 and at $\tau > 0$ begins to heat up under the action of the heat flux of radiation q of the laser.

4. In metals (conductors), the electromagnetic wave is exponentially attenuated in a very thin surface skin layer (~10^{-5} - 10^{-6} cm), with absorption occurring on conduction electrons. In laser processing of materials, the depth of heat penetration into the depth of the metal, although several orders of magnitude greater than the thickness of the skin layer, is practically adjacent to the surface of the material, and therefore in all calculations we will consider the heat source to be surface. We also assume that the energy of laser photons affecting the material is limited by the diameter of its focal spot d_f.

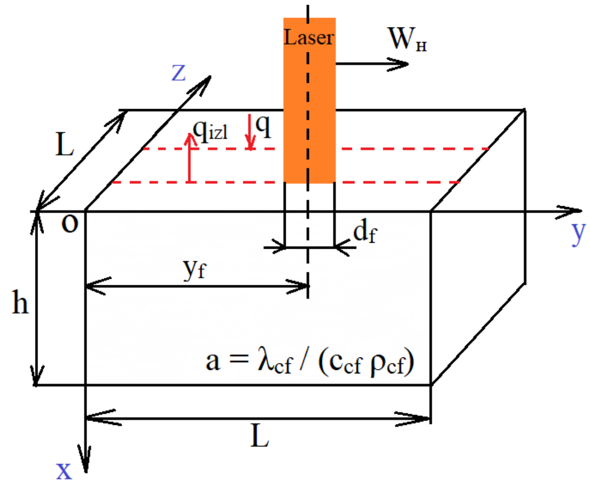

Fig. 3. Coordinate system and main dimensions of a two-layer plate during laser melting of a composite coating.

5. We consider that the temperature distribution in the metal plate is described by the energy equation considering phase transitions. We assume that metal evaporation, and hence the additional energy carried away for vaporization, can be neglected. When the metal surface is heated to a high temperature (T > 500°C), a significant heat flux of radiation q_{izl} to the environment occurs.

6. We will also consider that for the quenching problem our plate is cooled through the bottom face and side surfaces. Heat transfer occurs by setting the boundary conditions of the 3rd kind.

In order to achieve the target goal, the following tasks are set:

1. To create a mathematical model, calculation algorithm and software for modeling the unsteady thermal state of the plate at its laser heating, including the definition of:

- three-dimensional unsteady temperature field at given technological modes of laser processing, geometrical characteristics and thermophysical properties of the processed material;

- dynamics of the position of two-dimensional lines of the boundaries of the two-phase region for the liquidus and solidus of a metal at its melting and further solidification.

2. Computer modeling of unsteady thermal state of the processed metal and determination of the depth of its heating to the hardening temperature and possible penetration during its laser treatment.

Mathematical model of the thermal state of a metal plate during laser quenching

We will consider a three-dimensional mathematical model of the thermal state of a metal plate. The unsteady temperature distribution in the solid, two-phase and liquid regions is described by the energy equation taking into account the crystallization heat release according to the theory of quasi-equilibrium two-phase zone [7] (at $\tau > 0, 0 \le x \le h, 0 \le y \le L, 0 \le z \le L$)

$$c \cdot \rho_{ef} \cdot \frac{\partial T}{\partial \tau} - \rho_{ef} \cdot L_p \frac{\partial g}{\partial \tau} = \lambda_{ef} \cdot \left(\frac{\partial^2 T}{\partial x^2} + \frac{\partial^2 T}{\partial y^2} + \frac{\partial^2 T}{\partial z^2} \right),$$

where τ is time; $T(x, y, z, \tau)$ is temperature, g(T) is proportion of solid phase; ρ_{ef} is metal density; L_p is heat of fusion of metal.

Using substitution $\frac{\partial g}{\partial \tau} = \frac{\partial g}{\partial T} \frac{\partial T}{\partial \tau}$, the equation will take the following form:

$$\frac{\partial T}{\partial \tau} = \frac{\lambda_{ef}}{c_{ef} \rho_{ef}} \cdot \left(\frac{\partial^2 T}{\partial x^2} + \frac{\partial^2 T}{\partial y^2} + \frac{\partial^2 T}{\partial z^2} \right). \quad (1)$$

For the thermal problem, the amount of solid phase of the metal in the solidification interval will be determined by the model of the linear law $g(T) = \frac{(T_L - T)}{(T_L - T_S)}$, from which we can obtain $dg/dT = -1/(T_L - T_S)$, where T_L, T_S are the liquidus and solidus temperatures of the metal.

Depending on the chemical composition of the steel (for [C] < 2.14 %), the liquidus and solidus temperatures can be determined by the following empirical equations:

T_L = 1537 - (88.[C]+8.[Si]+5.[Mn]+4.[Cu]+5.[Cr]+ +25.[S]+30.[P]), °C;

T_S = 1537 - (200.[C]+16.[Si]+6.[Mn]+93.[P]+1100.[S]+ +1.7.[Cr]+3.9[Ni]), °C;

where square brackets indicate the concentration in percent of the corresponding chemical element in the steel composition.

The thermophysical properties of a metal are described by the following piecewise continuous functions:

$$\lambda_{ef} = \begin{cases} \lambda_{ML} \cdot \varepsilon_K & \text{at } T > T_L; & g = 0; \\ \lambda_{MS} g + \lambda_{ML}(1-g) & \text{at } T_S \le T \le T_L, & 0 < g < 1; \\ \lambda_{MS} & \text{at } T < T_S; & g = 1; \end{cases} \quad (2)$$

density

$$\rho_{ef} = \begin{cases} \rho_{ML}, & \text{at } T > T_L; \\ \rho_{MS} g + \rho_{ML}(1-g), & \text{at } T_S \le T \le T_S, & 0 < g < 1; \\ \rho_{MS}, & \text{at } T < T_S. \end{cases} \quad (3)$$

specific heat capacity

$$c_{ef}(T) = \begin{cases} C_{ML}, & \text{at } T > T_L; \\ C_{MS} g + C_{ML}(1-g) - L\frac{dg}{dT}, & \text{at } T_S \le T \le T_L \\ C_{MS}, & \text{at } T < T_S. \end{cases} \quad (4)$$

where λ_{ML}, λ_{MS} are thermal conductivity of liquid and solid metal; ρ_{ML}, ρ_{MS} are density of liquid and solid metal; C_{ML}, C_{MS} are specific heat capacity of liquid and solid metal; ε_K is increase of thermal conductivity coefficient due to circulation and turbulization of melt.

Eq. (1) can be written in the following form:

$$\frac{\partial T}{\partial \tau} = a_{ef}(T) \cdot \left(\frac{\partial^2 T}{\partial x^2} + \frac{\partial^2 T}{\partial y^2} + \frac{\partial^2 T}{\partial z^2} \right), \quad (5)$$

where the effective diffusivity as a function of temperature is $a_{ef}(T) = \frac{\lambda_{ef}(T)}{\rho_{ef}(T) \cdot C_{ef}(T)}$. Eq. (5) in this formulation is suitable for describing the entire remelting metal as a whole, without distinguishing the boundaries of solid, two-phase and liquid zones.

To solve the differential Eq. (5) it is necessary to supplement it with boundary conditions.

At the initial moment of time (at $\tau = 0$) we consider that the temperature in all points of the metal is the same ($\tau = 0$)

$$T(x, y, z, 0) = t_0. \quad (6)$$

Boundary conditions (at $\tau > 0$).

On the bottom surface of the plate we have a boundary condition of the 3rd kind (at $0 \le y \le L$, $0 \le z \le L$)

$$-\lambda_{ef} \cdot \left. \frac{\partial T}{\partial x} \right|_{x=h} = \alpha \cdot (T - t_g), \quad (7)$$

where α is heat transfer coefficient from the plate to the coolant, t_g is coolant temperature (air or water).

On the left and right side surfaces of the plate (at $0 \le x \le h, 0 \le z \le L$)

$$-\lambda_{ef}\cdot\frac{\partial T}{\partial y}\bigg|_{y=0}=\alpha\cdot(T-t_g)$$

$$-\lambda_{ef}\cdot\frac{\partial T}{\partial y}\bigg|_{y=L}=\alpha\cdot(T-t_g) \qquad (8)$$

On the front and back surfaces of the plate (at $0 \le x \le h$, $0 \le y \le L$)

$$-\lambda_{ef}\cdot\frac{\partial T}{\partial y}\bigg|_{z=0}=\alpha\cdot(T-t_g)$$

$$-\lambda_{ef}\cdot\frac{\partial T}{\partial y}\bigg|_{z=L}=\alpha\cdot(T-t_g) \qquad (9)$$

On the upper surface of the plate we have a boundary condition of the 2nd kind (at $0 \le y \le L$, $0 \le y \le L$)

$$-\lambda_{EF}\cdot\frac{\partial T}{\partial x}\bigg|_{x=0}=\xi\cdot q-q_{izl}(T)=q_{\Sigma}(T) \quad , \qquad (10)$$

where q is heat flux from the laser radiation; q_{izl} is heat radiation flux from the heated surface to the environment, and in the area of the laser spot impact is $\xi = 1$, in the rest of the area is $\xi = 0$.

Knowing at each moment of time τ the coordinate of the laser spot center $(0, y_f, z_f)$ it is possible to determine the area of heat flux impact on the metal surface:

$$y_f - r_f \le y_0 \le y_f + r_f, \quad z_0 = \pm\sqrt{(y_0-y_f)^2-r_f^2} \quad .$$

Photons falling on the metal have Maxwell distribution, so the heat flux density in the focal spot obeys the Gauss curve $q = A.I_n.exp(-r^2/r_f^2)$, where $A=1-R$ is the surface absorption coefficient of the metal, R is the coefficient of reflection of radiation by the surface, I_n is the maximum laser power density on its axis (at $r = 0$); and the average heat flux density in the focal spot is $\bar{q} = P_0/(\pi.r_f^2) \approx 0.747.\ I_n$, where P_0 is the laser radiation power. It is possible to use a simplified dependence of the average heat flux propagating into the depth of the material when exposed to the laser in the area of the focal spot $q=\frac{A\cdot P_H\cdot\eta}{\pi\cdot r_f^2}$, where η is the efficiency of the laser as a fraction of radiation from the power consumption P_H [8].

When a metal surface is heated to a high temperature ($T > 500$°C), heat flux is radiated from the surface to the surrounding environment

$$q_{izl}(T_{SURF})=E_R\cdot\sigma\left[\left(\frac{T_{SURF}+273}{100}\right)^4-\left(\frac{t_{ENV}+273}{100}\right)^4\right], \qquad (11)$$

where $\sigma = 5.7$ W m^{-2} K^{-4} - Stefan-Boltzmann constant;

$E_R=\frac{1}{1/\varepsilon_\kappa+1/\varepsilon-1}$ - the reduced degree of blackness, ε_κ, ε are degree of blackness of the metal surface and surrounding surfaces, respectively;

T_{SURF} and t_{ENV} are the temperature of the plate surface and the environment, respectively, °C.

RESULTS AND DISCUSSION

When conducting computer modeling, we will take the largest distance x_{fus}, where the maximum temperature is equal to the liquidus temperature of the metal, as the depth of maximum layer penetration. For the depth of the hardened layer we will take the largest distance x_{all}, where the hardening temperature T_{quen} was observed.

When considering the differential Eq. (5) with boundary conditions (6 - 11), exact solution methods encounter great difficulties. In these cases, one has to turn to some or other numerical solution methods.

The most used numerical methods are finite difference or grid methods. It is based on the replacement of derivatives by their approximate value expressed through differences of function values in separate discrete points - grid nodes. As a result of such transformations, the differential equation is replaced by an equivalent finite difference relation, the solution of which is reduced to the solution of a system of linear algebraic equations.

The advantages of the finite difference method include its high versatility, e.g., much higher than that of analytical methods. The application of this method is often characterized by the relative simplicity of the construction of the solving algorithm and its software implementation. It is often possible to parallelize the solving algorithm.

The disadvantages of the method include: the problematic nature of its use on irregular meshes; very rapid growth of computational labor intensity with increasing problem dimensionality (increasing the number of unknown variables); and the complexity of analytical study of the properties of the difference scheme.

In general, the finite difference method includes three main steps:

1) the stage of constructing a grid of nodal values of the desired function in the solution domain;

2) the stage of constructing on the basis of the initial differential equation a system of finite-difference

equations describing their functional relations between neighboring nodes of the grid;

3) the stage of solving the system of finite-difference equations with n unknowns using one of the numerical methods.

The number of n unknowns (or the order of solutions of the system) corresponds to the number of node values in which the value of the desired function is determined.

Let us introduce a space-time grid in the solution domain under consideration: $i = 1, 2, \dots N$, $j = 1, 2,\dots M$; $l = 1, 2,\dots LL$; $k=0, 1, 2,\dots K$; $x_i = i.\Delta x$, $y_i = j.\Delta y$ $z_i = l.\Delta z$, $\tau_k = k.\Delta\tau$, in general case $\Delta x \neq \Delta y \neq \Delta z$, where $(N–1)$, $(M–1)$, $(LL–1)$ are the number of partitions by x, y, z coordinates, respectively; K is the number of partitions by time. The grid has constant steps in x, y, z and τ, $\Delta x = h / (N - 1)$; $\Delta y = L / (M - 1)$, $\Delta z = L / (LL - 1)$. We replace the continuous temperature function by a grid function $T^k_{i,j,l} = T(x_i,y_j,z_l,\tau_k)$, .

To calculate the temperature field, we use the coordinate splitting scheme. At each time step, we will introduce an intermediate step where we will record a one-dimensional approximation along one of the spatial directions. The three-dimensional problem under consideration is “split” into a sequence of one-dimensional problems along each of the coordinates. The approximation errors of the intermediate layers are destroyed during summation.

To solve equation (5) for metal heating, we use the splitting scheme with application of the longitudinal-transverse scheme [9], which leads to an unconditionally stable locally one-dimensional scheme

$$\frac{T^{k+1/3}_{i,j,l}-T^{k}_{i,j,l}}{\Delta\tau/3} = a^k_{i,j,l}\left(\frac{T^{k+1/3}_{i+1,j,l}-2\cdot T^{k+1/3}_{i,j,l}+T^{k+1/3}_{i-1,j,l}}{\Delta x^2}\right), \quad (12)$$

$$\frac{T^{k+2/3}_{i,j,l}-T^{k+1/3}_{i,j,l}}{\Delta\tau/3} = a^{k+1/3}_{i,j,l}\cdot\left(\frac{T^{k+2/3}_{i,j+1,l}-2\cdot T^{k+2/3}_{i,j,l}+T^{k+2/3}_{i,j-1,l}}{\Delta y^2}\right) \quad (13)$$

$$\frac{T^{k+1}_{i,j,l}-T^{k+2/3}_{i,j,l}}{\Delta\tau/3} = a^{k+2/3}_{i,j,l}\cdot\left(\frac{T^{k+1}_{i,j,l+1}-2\cdot T^{k+1}_{i,j,l}+T^{k+1}_{i,j,l-1}}{\Delta z^2}\right), \quad (14)$$

where $a^k_{i,j,l} = \frac{\lambda^k_{i,j,l}}{C^k_{EF\ i,j,l}\cdot\rho^k_{i,j,l}}$, $a^{k+1/3}_{i,j,l} = \frac{\lambda^{k+1/3}_{i,j,l}}{C^{k+1/3}_{EF\ i,j,l}\cdot\rho^{k+1/3}_{i,j,l}}$, $a^{k+2/3}_{i,j,l} = \frac{\lambda^{k+2/3}_{i,j,l}}{C^{k+2/3}_{EF\ i,j,l}\cdot\rho^{k+2/3}_{i,j,l}}$.

The system of linear algebraic equations (SLAE) for Eq. (12) can be represented as

$$A_1\cdot T^{k+1/3}_{i-1,j,l} - B_1\cdot T^{k+1/3}_{i,j,l} + C_1\cdot T^{k+1/3}_{i+1,j,l} = D_1, \quad (15)$$

where $A_1 = Fo^k_{i,j}$, $B_1 = 2\cdot Fo^k_{i,j}+1$, $C_1 = Fo^k_{i,j}$,

$D_1 = -T^k_{i,j,l}$, $Fo^k_{i,j} = \frac{a^k_{i,j,l}\cdot\Delta\tau}{3\cdot\Delta x^2}$.

Similarly, we can write SLAEs for Eq. (13) and (14).

Solving three SLAEs sequentially, we obtain the value of functions $T^{k+1}_{i,j,l}$, which differs from the true value $T(x, y, z, \tau)$ of the problem solution by the value $O(\Delta\tau^2)$. In this case, the process of solving a three-dimensional problem is replaced by the process of sequentially solving three one-dimensional problems.

The described difference splitting scheme has advantages in the sense of simplicity and clarity of the problem to be solved and relatively small amount of calculations.

Each of the SLAEs was solved by the run method; the algorithm of this method includes two stages.

1. For all i = 2, 3, , N -1 we determine the coefficients (direct run)

$$\alpha_i = \frac{A_i}{B_i - C_i\cdot\alpha_{i-1}};\ \beta_i = \frac{C_i\cdot\beta_{i-1}-D_i}{B_i - C_i\cdot\alpha_{i-1}}, \quad (16)$$

at the same time, we consider α_1 and β_1 to be known from the left boundary condition as well.

2. For all i = (N -1), ..., 2, 1, we determine the temperatures (backpropagation)

$$T_i = \alpha_i.T_{i+1} + \beta \quad (17)$$

at the same time, we consider T_N known from the right boundary condition (BC).

Let us consider the algorithm for discretization of initial and boundary conditions.

For the initial temperature distribution (6) for the entire computational domain we have $T_{i,j,l} = t_0$.

At the x-propagation on the left boundary, a BC of the 2nd kind acts on the left boundary. From expression (17) we have $T_1 = \alpha_1 T_2 + \beta_1$, from expression (13) - $\lambda_{ef}\cdot\frac{T_1-T_2}{\Delta x} = q_\Sigma$, solving these equations together, we obtain (at i = 1, 2,... N) $\alpha_1 = 1$, $\beta_1 = \frac{\Delta x\cdot q_\Sigma}{\lambda_{ef}}$.

When running along x at the right boundary, we have the BC of the 3d kind.

At the coolant boundary, from (8) we have

$\lambda_{ef}\cdot\frac{T_{N-1}-T_N}{\Delta x} = \alpha.(T_N - t_g)$.

Substituting the expression based on (17):
$T_{N-1} = \alpha_{N-1} T_N + \beta_{N-1}$, we get

$$T_N = \frac{\beta_{N-1} + \phi \cdot t_g}{1 - \alpha_{N-1} + \phi},$$

where $\phi = \alpha.\Delta x/\lambda_{ef}$.

When running along y at the left boundary, we have a BC of the 3d kind.

At the coolant boundary from (9) we have $\lambda_{ef} \cdot \frac{T_2 - T_1}{\Delta y} = \alpha\ .\ (T_1 - t_g)$. From expression (17 we have $T_1 = \alpha_1\ .\ T_2 + \beta_1$, we obtain (at j = 1, 2,... M)
$\alpha_1 = \frac{1}{1+\phi}$, $\beta_1 = \frac{\phi}{1+\phi} \cdot t_g$, where $\phi = \Delta y\ .\ \alpha/\lambda_{ef}$.

When running along y on the right boundary we have the BC of the 3d kind.

At the coolant boundary from (10) we have $\lambda_{ef} \cdot \frac{T_{M-1} - T_M}{\Delta y} = \alpha \cdot (T_M - t_g)$.

Substituting the expression based on (17) $T_{M-1} = \alpha_{M-1} T_M + \beta_{M-1}$, we obtain $T_N = \frac{\beta_{M-1} + \phi \cdot t_g}{1 - \alpha_{M-1} + \phi}$, where $\phi = \alpha\ .\ \Delta y\ /\lambda_{ef}$.

When running along z, the boundary conditions on the left and right boundaries are written similarly.

Based on the considered mathematical model, the computer program “Laser_hardening_of_metal” was created in the Matlab environment. To carry out computer modeling, data on the thermophysical properties of the tempered steel were collected. Tabular thermophysical properties of 40X steel were taken from [10] and based on them, equations for approximating the density, specific heat capacity and thermal conductivity coefficient of solid (at $20 \le t \le 1100$°C) and liquid steel, respectively, were obtained:
$\rho_{MS}(t)$ - 7830 - 0.283.t - 3.23.$10^{-5}t^2$, ρ_{ML} = 7040, (kg m^{-3});
$\tilde{N}_{MS}(t)$ = 432 + 0.371.t - 1.05 . $10^{-4}t^2$,
$\tilde{N}_{ML}$ = 825 (J kg^{-1} K^{-1});
$\lambda_{MS}(t)$ = 45.8 + 5.12.10^{-3}.t - 8.19.$10^{-5}t^2$ + 5.79.$10^{-8}t^3$,
λ_{ML} = 39 (W m^{-1} K^{-1}).

The melting heat of steel $L_p = 2.7 \cdot 10^5$ J kg^{-1}. Calculations were carried out with the following initial data: L = 50 mm; h = 6 mm; t_0 = 20°C; t_{oc} = 15°C; t_g = 15°C; A = 0.74; n = 0.6; e_k = 0.7; e = 0.85; P_h = 1200 W; r_f = 1 mm; W_h = 12.5 mm s^{-1}. The calculated value is T_L = 1488°C, T_S = 1411°C.

By means of computer simulation, the temperature fields of a metal plate are obtained when exposed to a laser beam and simultaneously cooled with water. The results of the program are presented in the form of tables, diagrams and graphs. Under the selected remelting conditions, the average heat flux in the focal spot area was q ≈ 17 kW cm^{-2}. Calculations were performed for cooling conditions of a metal plate immersed in water $\alpha = 10^3$ W m^{-2} K^{-1} and conditions of intensive cooling with water $\alpha = 10^4$ W m^{-2} K^{-1}. Fig. 4a, b shows diagrams of temperature distribution at time points τ = 1.92 s (the coordinate of the center of the focal spot is in the middle of the plate y_f = L/2 = 25 mm) and in Fig. 4b, d at the time after the passage of the beam τ = 3.84 s. Seven isotherms are given, with 7 and 6 being the liquidus and solidus temperatures of the metal, respectively, and 5 being the tempering temperature of T_{quen}. At the same time, the maximum temperature in the focal spot is about 3160°C.

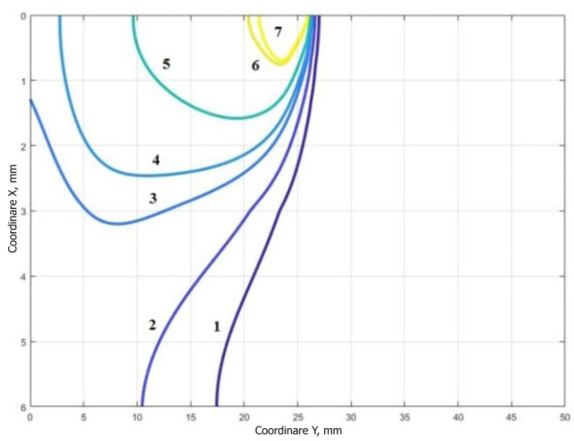

a)

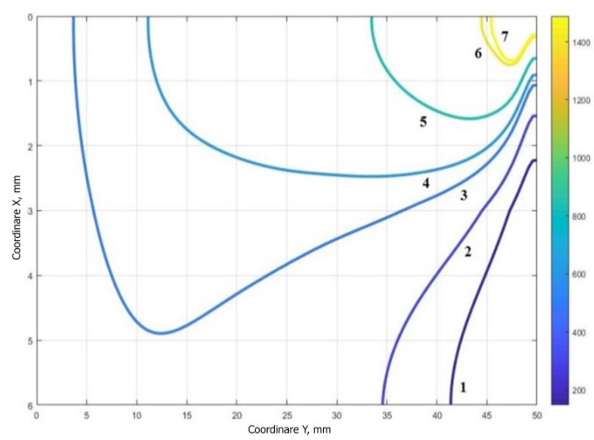

b)

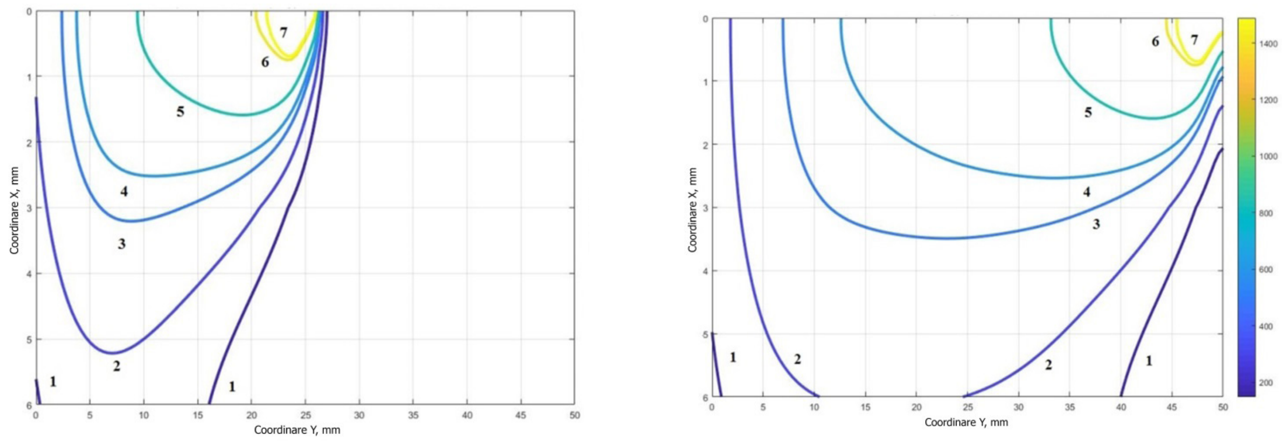

c) d)

Fig. 4. Diagram of the temperature distribution at the time when the laser beam passes through half of the plate (a, c) and at the time of its complete passage (b, d).

The penetration depth of the metal was about 0.7 mm, the hardening depth of the steel was about 1.5 mm.

It was found that the maximum temperature at a given depth is set after about 0.5 - 0.7 seconds and then practically does not change over the course of the entire passage. So at a distance from the surface 0.5 mm $T_{max} \approx 2000°C$, at a distance from the surface of 1 mm $T_{max} \approx 1200°C$.

The results are shown under the condition of cooling a metal plate immersed in water $\alpha = 10^3$ W m^{-2} K^{-1} (a, b) and under the condition of intensive cooling with water $\alpha = 10^4$ W m^{-2} K^{-1} (c, d). The figures on the graphs correspond to isotherms: 1 - 150°C; 2 - 300°C; 3 - 500°C; 4 - 600°C; 5 - T_{quen} = 830°C; 6 - T_S = 1411°C; 7 - T_L = 1488°C.

CONCLUSIONS

Based on the assumptions and limitations considered, a mathematical model is formulated that represents the boundary value problem of calculating the non-stationary thermal state of a tempered metal plate and determining the depth of its heating and possible penetration when a laser beam moves along its surface using a parallel line strategy. A numerical algorithm is proposed that allows approximating the boundary value problem of the warm state of the plate, determining the depth of the hardened layer and rational technological parameters of metal cooling. Based on the considered mathematical model and numerical algorithm, a computer program "Laser_hardening_of_metal" has been created in the Matlab environment, which allows computer modeling of the warm state of a plate made of a given grade of steel and determining the depth of the hardened layer, as well as choosing rational technological parameters of laser beam power, scanning speed and strategy, and metal cooling. The calculation of temperature fields in a 40X steel plate when exposed to a laser beam with two modes of cooling it with water is shown. The developed software will make it possible to predict the rational technological parameters of quenching for various steels when using the KUKA KR120 robotic installation.

Acknowledgments

The work was supported financially by the Russian Federation represented by the Ministry of Science and Higher Education of the Russian Federation, project number No. 075-15-2022-1243.

Authors' contributions: *S.L.: Writing, Review, Editing, Data Curation; E.N.: Investigation, Methodology, Writing Original Draft; I.Y.: Methodology, Writing Original Draft, Resources, Software; Y.L.: Writing Original Draft, Formal analysis; M.S.: Conceptualization, Investigation, Methodology, Supervision, Project administration, Funding acquisition; E.T.: Investigation, Methodology, Validation; E.P.: Visualization, Formal analysis, S.E.: Writing, Review, Editing, Resources.*

REFERENCES

1. M.V. Voevodin, T.A. Mitroshkina, A.Ya. Dmitriev, Modeling and analysis of laser welding technology for aircraft engine blade repair, Quality and Life, 2020, 2, 6, 82-87, (in Russian).
2. M.S. Serdeczny, Laser welding of dissimilar materials - simulation driven optimization of process parameters, IOP Conference Series: Materials Science and Engineering, 2023, 1281, 012018. https://doi.org/10.1088/1757-899X/1281/1/012018
3. I.I. Marhoon, M.A. Abdulrehman, A.A. Salman, Evaluating study for laser-based welding for aluminum alloys using CFD modeling, Journal of Mechanical Engineering Research and Developments, 2021, 44, 6, 71-81.
4. L.S. Petrova, Ya.V. Kryukova, Mathematical modeling of the process of high-intensity heating of bodies with coatings during surface treatment with laser radiation, Izvestia Transsib, 2018, 1, 118-129, (in Russian).
5. N. Maharjan, N. Wu, W. Zhou, Hardening Efficiency and Microstructural Changes during Laser Surface Hardening of 50CrMo4 Steel, Metals, 2021, 11, 2015. https://doi.org/10.3390/met11122015
6. Y.M. Klimkov, V.S. Mayorov, M.V. Sneddon, Interaction of laser radiation with matter, Moscow: MIIGAiK, 2014, (in Russian).
7. E.V. Timchenko, P.E. Timchenko, Interaction of laser radiation with matter, Samara, Samara State Aerospace University, 2014, (in Russian).
8. H.-S. Roh, Internal energy transfer theory for thermodynamic non-equilibrium, quasi-equilibrium, and equilibrium, International Journal of Heat and Mass Transfer, 2014, 78, 778-795.
9. L.I. Turchak, P.V. Plotnikov, Fundamentals of numerical methods, Moscow: Fizmatlit, 2002, (in Russian).
10. V.G. Sorokin, M.A. Gervasyev, Guide of steels and alloys, Moscow, Intermet Engineering, 2001.